UAV-Based Antenna Measurements: Improvement of the Test Source Frequency Behavior

Fabio Paonessa
Istituto di Elettronica e di Ingegneria dell'Informazione e delle Telecomunicazioni (IEIIT)
Consiglio Nazionale delle Ricerche (CNR)
Turin, Italy
fabio.paonessa@ieiit.cnr.it

Giuseppe Virone
Istituto di Elettronica e di Ingegneria dell'Informazione e delle Telecomunicazioni (IEIIT)
Consiglio Nazionale delle Ricerche (CNR)
Turin, Italy
giuseppe.virone@ieiit.cnr.it

Pietro Bolli
Osservatorio Astrofisico di Arcetri (OAA)
Istituto Nazionale di Astrofisica (INAF)
Firenze, Italy
pbolli@arcetri.inaf.it

Giuseppe Addamo
Istituto di Elettronica e di Ingegneria dell'Informazione e delle Telecomunicazioni (IEIIT)
Consiglio Nazionale delle Ricerche (CNR)
Turin, Italy
giuseppe.addamo@ieiit.cnr.it

Stefania Matteoli
Istituto di Elettronica e di Ingegneria dell'Informazione e delle Telecomunicazioni (IEIIT)
Consiglio Nazionale delle Ricerche (CNR)
Pisa, Italy
stefania.matteoli@ieiit.cnr.it

Oscar A. Peverini
Istituto di Elettronica e di Ingegneria dell'Informazione e delle Telecomunicazioni (IEIIT)
Consiglio Nazionale delle Ricerche (CNR)
Turin, Italy
oscar.peverini@ieiit.cnr.it

***Abstract*—Drone-based radiation pattern measurements require the knowledge of the whole test-source radiation pattern in order to reach the expected measurement accuracy. However, the radiation pattern of the onboard antenna can be highly distorted by the metal frame of the vehicle, particularly in the VHF and UHF bands, showing highly resonant behaviors. This paper presents a preliminary analysis aimed to highlight such behavior and adopt compatible solutions to minimize or avoid the pattern distortion in the frequency of interest.**

Keywords—Radiation pattern, antenna measurements, Unmanned Aerial Vehicle, Drones

I. INTRODUCTION

Nowadays, the modern technology of the Unmanned Aerial Vehicles (UAVs) provides versatile tools to perform in-situ antenna measurements. UAVs can carry radio-frequency transmitters allowing to easily characterize ground based receiving antenna systems in their real installation conditions, at a low-cost and high flexibility [1]-[6]. UAV-mounted test-sources have been already used to verify, both in near-field and far-field, the electromagnetic models of new-generation radio telescopes based on the phased array technology and to perform the array calibration [7]-[11]. According to the data processing procedure of [12], an accurate knowledge of the test-source radiation pattern is one of the most important requirements to reach the expected accuracy. In [13], the problem of the electromagnetic modeling of the whole test-source (i.e. the antenna mounted on the UAV) and its experimental verification have been addressed. It was demonstrated that the interaction between the UAV and the onboard antenna can produce an unwanted behavior in the test-source radiation pattern at particular frequencies. This problem is particularly significant due to the fact that the source antenna is generally mounted on general-purpose commercial drones (see Fig. 1), close to the vehicle frame in order not to lower the drone center of mass. In this work, a parametric analysis is carried out to highlight this effect and adopt suitable solutions.

Fig. 1. The test-source consisting in a multicopter carrying a frequency synthesizer and a dipole antenna.

II. PARAMETRIC ANALYSIS OF THE UAV-MOUNTED DIPOLE

The UAV hereby considered is a commercial 3D Robotics X8+ which has been customized in order to carry a frequency synthesizer and a dipole antenna (see Fig. 1). The vehicle is made of several dielectric and aluminum parts. The electromagnetic model of the whole test-source (see illustration in Fig. 2a) only contains the metal parts since the dielectric ones, e.g. the legs, are thin and have low permittivity. The metal grid beneath the copter arms, visible in Fig. 1 and 2, has been modeled as a solid plate since the mesh size is definitely smaller than the wavelength at all the considered operative frequencies (70-350 MHz). The maximum copter width

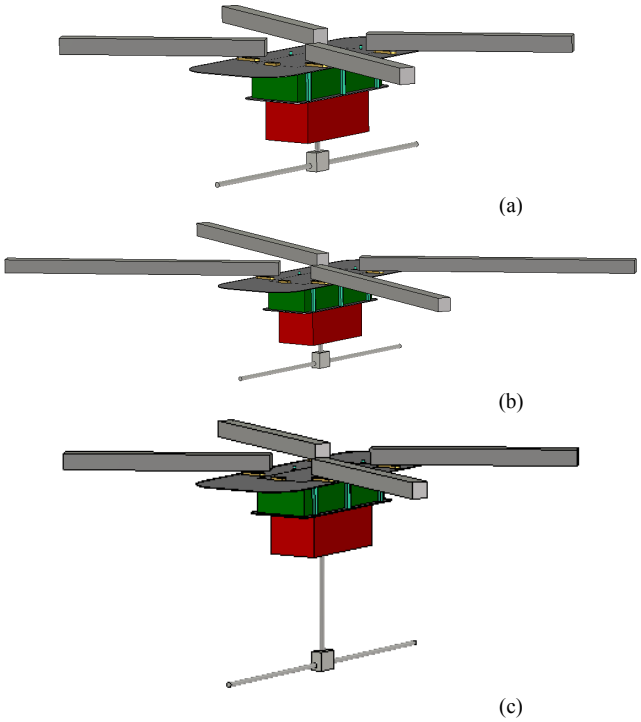

Fig. 2. Electromagnetic model of the test-source, which includes the four metal arms, the underlying grid, the battery compartment (green), the RF synthesizer (red) and the dipole: (a) original version with short arms, which corresponds to the test-source shown in Fig. 1; (b) alternative version with extended arms; (c) second alternative version where the distance between the dipole and the frequency synthesizer has been increased to 13.4 cm.

(motor-to-motor) is about 50 cm. The frequency generator box is 12×6×5 cm^3. The dipole is connected to the transmitter through a wideband balun housed in a metal box of 2.4×2×1.4 cm^3. The distance between the TX box and the balun is 3.35 cm. The monopole pairs are made of replaceable fixed-length rods, which are kept in the right alignment by dielectric flanges fixed to the synthesizer box.

The radiation pattern of the overall test-source has been computed (full-wave simulations) at several operative frequencies between 70 and 350 MHz. It should be pointed out that the length of the dipole has been tuned at each operative frequency in order to achieve a good impedance matching (minimum reflection coefficient). This strategy mimics the behavior of an optimum broadband antenna. The objective of this analysis was in fact only focused on the radiation performance in presence of the UAV frame. The corresponding length of the monopoles ranges from 18 cm (350 MHz) to 100 cm (70 MHz). The obtained nadir directivity versus the frequency is reported in Fig. 3 (blue curve). As already highlighted in [11], at the lowest frequencies (100 MHz and less) the effect of the metal frame on the radiation pattern is negligible, and the nadir directivity almost coincides to that of a half-wavelength dipole. At the highest frequencies, instead, the frame operates as a small ground plane increasing the nadir directivity.

It is interesting to notice the behavior at approximately 230 MHz (blue curve). At this frequency, the strong interaction

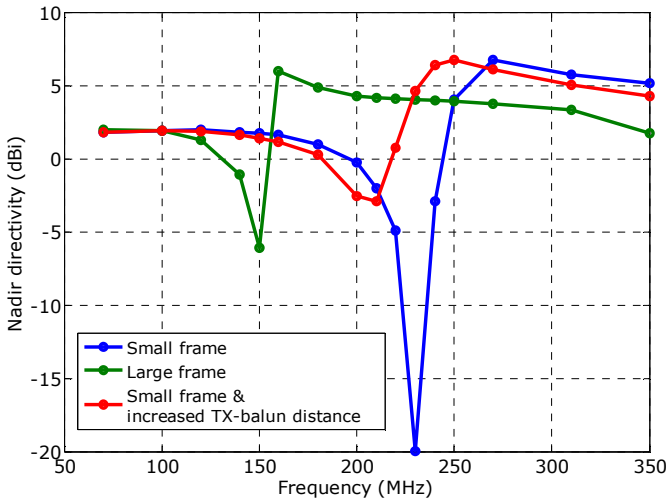

Fig. 3. Computed nadir directivity for the test-source versus the operative frequency. Original copter frame (blue curve); modified copter frame with longer arms (green curve). Original frame with increased distance between dipole and transmitter (red curve).

between the metal frame and the dipole produces a very low directivity toward the nadir. Such condition is not desirable in terms of signal-to-noise ratio of the measurement system. As a matter of fact, it prevents performing measurements with the expected accuracy in the proximity of 230 MHz. Moreover, even at the adjacent frequencies, such a narrow-band behavior is critical in terms of the overall knowledge of the UAV-mounted test source, with particular reference to the radiation pattern sensitivity with respect to the overall model uncertainties, including both geometry and material properties. It should be also noted that an experimental characterization of the test source radiation pattern is not straightforward at this frequency, therefore, numerical models have been always used to performed the measurement post-processing in [1],[7]-[13].

Other UAVs with compatible payload capability will have similar shape and dimensions. Therefore, even with a different vehicle, the issue will be present within the band of interest. Therefore, the vehicle frame dimensions have been changed in order to vary its resonance frequency. The frame width of the model illustrated in Fig. 2b has been extended from about 50 cm to 80 cm. As expected, the results in this case (green curve of Fig. 3) show that the resonance frequency has been reduced, from 230 MHz to about 150 MHz. The frequency separation is sufficient to allow covering the whole frequency range with one of the two UAV frames. On the other hand, it is required to make use of two different vehicles or to adopt a more complex platform where the vehicle arms can be extended.

Another solution has been investigated. The distance between the dipole and the frequency synthesizer (see model in Fig. 2c) has been increased, in order reduce the coupling with the UAV frame. Such solution is easy to implement, however it will make more difficult to keep the dipole firmly aligned. Moreover, the allowable legs length is limited due to stability, weight and compactness reasons. The simulated results (red curve of Fig. 3) show that the null at the resonance frequency is

effectively reduced with a distance of 13.4 cm. At about 210 MHz, the test-source pattern is still fairly directive toward the zenith, however, depending on the transmitted power and the receiver dynamic range, it can be considered acceptable.

III. Model Verification

This section discusses the experimental validation of the model used in the parametric simulations reported above. Due to the impossibility to directly measure the test-source radiation patterns in anechoic chamber at such low frequencies, the simulated patterns have been verified outdoor in combination with simple reference antennas placed on the ground. The test-source shown in Fig. 1 has been used. Fig. 4 reports the measured received power patterns (solid lines) obtained at 250 MHz with a log-periodic PMM LP-02 antenna pointed at zenith. The UAV flights consisted in two constant-height rectilinear scans above the antenna under test, which provided the quasi-*E/H*-plane cuts. This experiment represents a verification of all the contributions, i.e. the test-source pattern, the reference antenna pattern and the variable path loss. Measured (solid lines) and simulated data (dashed lines) are consistent within 0.3 dB and the main discrepancy is above ±50° of zenith angle in the *H*-plane. The discrepancy can be explained by the simulation accuracy for both the test-source and the ground antenna (EM model and soil parameters).

IV. Conclusion

An accurate electromagnetic model of the test-source is mandatory for UAV-based antenna measurement. The interaction between the UAV metal frame and the onboard antenna can produce a significant distortion in the test-source radiation pattern at particular frequencies. This work highlighted such a behavior for a test-source operating in the band 50-350 MHz. The proposed solutions aim to limit the interaction between the onboard antenna and the metal parts, compatibly with the vehicle constraints in terms of size and weight. In this framework, a comprehensive design of a test-source for UAV-based antenna measurements should consider not only the onboard antenna but also the vehicle properties both from the point of view of flight dynamics and electromagnetic properties.

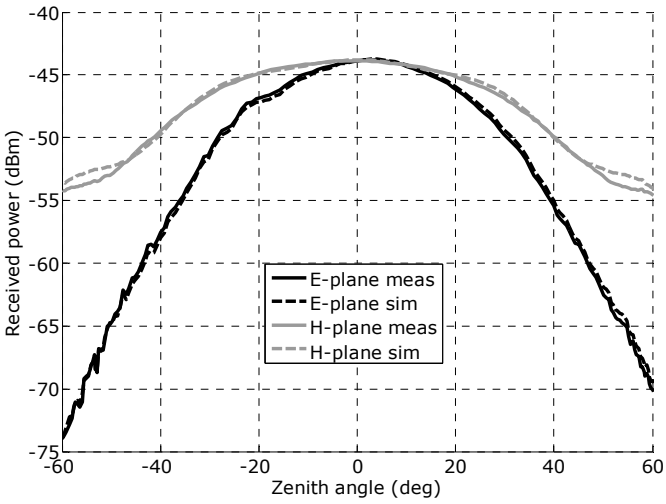

Fig. 4. Received power pattern at 250 MHz, which is proportional to both the test-source and the antenna-under-test patterns: E-plane measurement (solid black), E-plane simulation (dashed black), H-plane measurement (solid gray), H-plane simulation (dashed gray).

References

[1] G. Virone et al., "Antenna pattern verification system based on a micro unmanned aerial vehicle (UAV)," *IEEE Antennas and Wireless Propagation Letters*, vol. 13, pp. 169–172, Jan. 2014.

[2] M. García-Fernández et al., "Antenna Diagnostics and Characterization Using Unmanned Aerial Vehicles," IEEE Access, vol. 5, pp. 23563-23575, 2017.

[3] T. Fritzel, R. Strauß, H. J. Steiner, C. Eisner and T. Eibert, "Introduction into an UAV-based near-field system for in-situ and large-scale antenna measurements (Invited paper)," 2016 IEEE Conference on Antenna Measurements & Applications (CAMA), Syracuse, NY, 2016, pp. 1-3.

[4] C. Chang et al., "Beam calibration of radio telescopes with drones," *Publications of the Astronomical Society of the Pacific*, vol. 127, no. 957, 2015.

[5] F. Üstüner et al., "Antenna radiation pattern measurement using an unmanned aerial vehicle (UAV)," *General Assembly and Scientific Symposium (URSI GASS)*, 2014 XXXIth URSI, Beijing, 2014, pp. 1-

[6] L. Washburn, E. Romero, C. Johnson, B. Emery and C. Gotschalk, "New applications for autonomous aerial vehicles (drones) in coastal oceanographic research", Ocean Sciences Meeting 21-26 Febraury 2016, New Orleans, Louisiana, USA.

[7] G. Virone et al., "Strong Mutual Coupling Effects on LOFAR: Modeling and In Situ Validation," *IEEE Transactions on Antennas and Propagation*, vol. 66, no. 5, pp. 2581–2588, May 2018.

[8] P. Bolli et al., "Near-Field Experimental Verification of the EM Models for the LOFAR Radio Telescope," *IEEE Antennas and Wireless Propagation Letters*, vol. 17, no. 4, pp. 613–616, Apr. 2018.

[9] E. de Lera Acedo et al., "SKA Aperture Array Verification System: Electromagnetic modeling and beam pattern measurements using a micro UAV", *Experimental Astronomy*, vol. 45, no. 1, pp. 1–20, Mar. 2018.

[10] P. Bolli et al., "From MAD to SAD: the Italian experience for the Low Frequency Aperture Array of SKA1-LOW," *Radio Science*, vol. 51, no. 3, pp. 160–175, Mar. 2016.

[11] G. Pupillo et al., "Medicina Array Demonstrator: Calibration and Radiation Pattern Characterization Using a UAV-Mounted Radio Frequency Source," *Experimental Astronomy*, vol. 39, no. 2, pp. 405–421, June 2015.

[12] G. Virone et al., "Antenna pattern measurements with a flying far-field source (hexacopter)," IEEE International Conference on Antenna Measurements and Applications (CAMA), Antibes Juan-les-Pins, France, Nov. 16-19, 2014.

[13] G. Virone et al., "Antenna pattern measurement with UAVs: Modeling of the test source," *2016 10th European Conference on Antennas and Propagation (EuCAP)*, Davos, Switzerland, Apr. 2016, pp. 1–3.